8.4 Equations of Particle Motion

To design particle collection devices and to predict their performance, engineers must be able to predict the trajectories of particles passing through the devices. The objective of this section is to establish equations that predict the trajectories of particles. As an aerosol particle moves through air, it disturbs the air, changing the velocity and pressure fields of the air flow. In addition, particles collide with each other and are influenced by each others' wakes. Exact analysis of particles moving in air is therefore nearly impossible, even for simple air flows, since the equations for the air flow and for each particle's trajectory are coupled. Fortunately, some simplifications are possible, which make the problem more tractable. Two major assumptions are made here:

1. Particles move independently of each other.
2. Particles do not influence the flow field of the carrier gas.

The first assumption is valid if two conditions are met: (a) particle collisions are infrequent and inconsequential, and (b) particles are not significantly affected when they pass through each others' wakes. A useful rule of thumb that quantifies these conditions for a monodisperse aerosol is that the average distance between particles is at least 10 times the particle diameter. Assuming that 8 particles are located at the corners of a cube of dimension L, one finds that $L/D_p > 10$ when

$$\boxed{\frac{4\pi\rho_p}{3c} = \frac{8}{(c_{number})D_p^{\,3}} > 1000} \qquad (8\text{-}51)$$

where c is the mass concentration of particles, ρ_p is the particle density, and $c_{number} = n_t/V$ is the ***particle number concentration***, defined as the total number of particles per unit volume of gas. Table 8.3 illustrates these upper limits and indicates that the particle number concentration has to be exceedingly large for the particles to influence each other. For water droplets (ρ_p = 1,000 kg/m^3), application of Eq. (8-51) leads to a particle mass concentration c = 4.2 kg/m^3, corresponding to the upper limit of 1,000 in Eq. (8-51). For most problems in indoor air pollution, particle concentrations of water and particulate pollutants are *hundreds* of times smaller than 4.2 kg/m^3. Consequently the first assumption above is clearly valid, and one can calculate the trajectory of one individual particle at a time.

The second assumption is more difficult to quantify. Large objects moving through air generate air flows due to displacement effects and the effects of aerodynamic wakes. For example, a pedestrian walking along the side of a road feels the "wind" created by a passing vehicle. The same effect can be experienced when a person walks past another person in otherwise quiescent air. Automobiles and people, however, are very large objects; particles usually associated with indoor air pollution are many orders of magnitude smaller. As shown below, most particles of interest to indoor

Table 8.3 Particle number concentrations beyond which particles influence each other.

D_p (μm)	c_{number} (particles/m^3)
1	8 x 10^{15}
10	8 x 10^{12}
100	8 x 10^{9}

air pollution move at extremely small speeds relative to the surrounding air, and therefore do not significantly alter the air flow field. The second assumption is critical to the analysis that follows. The approach is to first solve for the flow field of the carrier gas independently of the particles, and then to compute the particle trajectories through this "frozen" carrier gas flow field. Mathematically, the assumption is equivalent to an ***uncoupling*** of the equations.

The flow field of the carrier gas can be expressed analytically if one is so fortunate as to have a system of simple geometry, or it may be established experimentally and the data stored numerically. If an analytical expression for the velocity field exists, one can compute the particle trajectories explicitly. For most industrial applications only experimentally measured velocity data are available and a computer is needed to compute the particle trajectories.

An equation of motion for a particle can be derived from Newton's second law. Namely, particle mass times acceleration of the particle is equal to the vector sum of all the forces acting on the particle. Only two forces are considered here – gravitational force (net weight) and aerodynamic drag. Newton's second law is therefore

$$\boxed{m_{particle}\vec{a} = \sum \vec{F} = \vec{F}_{gravity} + \vec{F}_{drag}} \qquad (8\text{-}52)$$

Other forces, such as magnetic forces, etc., are ignored here.

8.4.1 Gravitational Force

The net gravitational force is equal to the weight of the particle minus the buoyancy force on the particle, where the buoyancy force is equal to the weight of the air displaced by the particle. For a spherical particle,

$$\boxed{\vec{F}_{gravity} = m_{particle}\vec{g} - m_{air}\vec{g} = \pi\frac{D_p^{\,3}}{6}\rho_p\vec{g} - \pi\frac{D_p^{\,3}}{6}\rho\vec{g} = \pi\frac{D_p^{\,3}}{6}\left(\rho_p - \rho\right)\vec{g}} \qquad (8\text{-}53)$$

where $\vec{g}$ is the acceleration of gravity, ρ is the density of the air, and ρ_p is the density of the particle. The density of a particle is typically of order 1,000 times greater than the density of air ($\rho_p >> \rho$). Thus the force of buoyancy on a particle is often neglected compared to its weight,

$$\boxed{\vec{F}_{gravity} = \pi\frac{D_p^{\,3}}{6}\left(\rho_p - \rho\right)\vec{g} \approx \pi\frac{D_p^{\,3}}{6}\rho_p\vec{g}} \qquad (8\text{-}54)$$

The approximation of Eq. (8-54) is *not* made in the material which follows, so that the equations are more general.

8.4.2 Aerodynamic Drag

Consider a particle moving at some arbitrary velocity $\vec{v}$ through air, at a location in which the air is moving at some other arbitrary velocity $\vec{U}$ along a streamline of the air flow. As the particle moves relative to the air, as in Figure 8.10, the air produces an ***aerodynamic drag force*** on the particle.

As indicated in the sketch, the aerodynamic drag force ($\vec{F}_{drag}$) acts in the direction of $-\vec{v}_r$, i.e. in the direction opposite to the velocity of the particle relative to the air. The net force on the particle is the vector sum of the gravitational force and the drag force, as also sketched in Figure 8.10. The particle in Figure 8.10 veers to the right and decelerates since the net force in this example is somewhat opposite to the particle's direction and to the right. For a sphere of diameter D_p, $\vec{F}_{drag}$ can be written as

$$\boxed{\vec{F}_{drag} = -c_D\frac{\rho}{2}\frac{\pi D_p^{\,2}}{4}\left(\vec{v} - \vec{U}\right)\left|\vec{v} - \vec{U}\right| = -c_D\frac{\rho}{2}\frac{\pi D_p^{\,2}}{4}\vec{v}_r\left|\vec{v}_r\right|} \qquad (8\text{-}55)$$

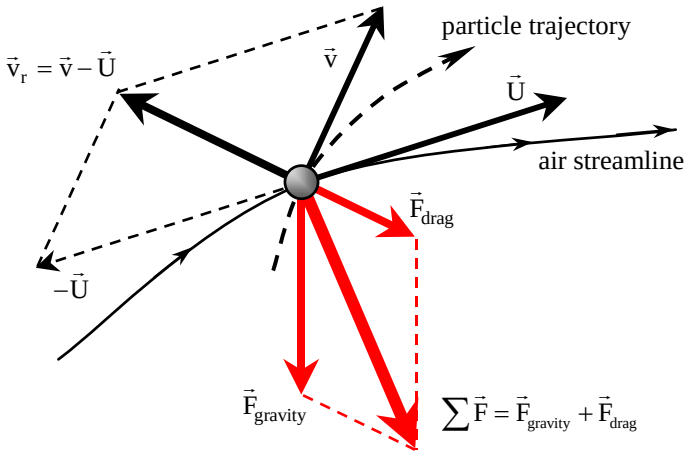

Figure 8.10 Particle moving through air, which is also moving; $\vec{U}$ is the air velocity and $\vec{v}$ is the particle velocity; gravitational force, drag force, and net force on the particle are shown.

where

- $\vec{U}$ = carrier fluid (air) velocity
- $\vec{v}$ = particle velocity
- $\vec{v}_r$ = ***relative velocity*** (particle velocity relative to the air),

$$\boxed{\vec{v}_r = \vec{v} - \vec{U} = \hat{i}\left(v_x - U_x\right) + \hat{j}\left(v_y - U_y\right) + \hat{k}\left(v_z - U_z\right) = \hat{i}v_{rx} + \hat{j}v_{ry} + \hat{k}v_{rz}} \qquad (8\text{-}56)$$

- $\left|\vec{v}_r\right| = \left|\vec{v} - \vec{U}\right| = v_r$ = ***magnitude of the relative velocity***, also called the ***relative speed***,

$$\boxed{\left|\vec{v} - \vec{U}\right| = \sqrt{\left(v_x - U_x\right)^2 + \left(v_y - U_y\right)^2 + \left(v_z - U_z\right)^2} = \sqrt{v_{rx}^{\,2} + v_{ry}^{\,2} + v_{rz}^{\,2}}} \qquad (8\text{-}57)$$

- c_D = ***drag coefficient*** for a sphere, based on projected frontal area

Figure 8.11 shows the drag coefficient for a sphere as a function of Reynolds number. Similar curves

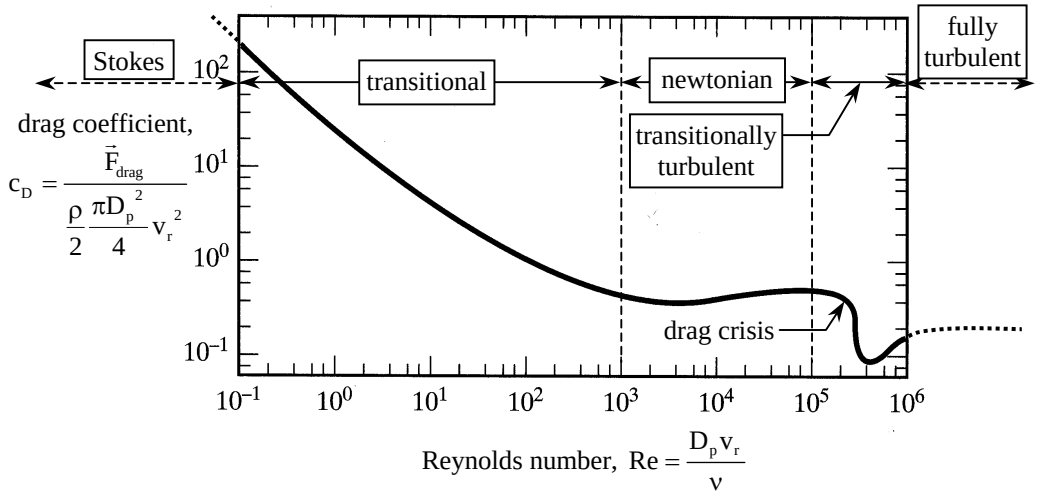

Figure 8.11 Drag coefficient of a sphere versus Re (redrawn from Incropera and DeWitt, 1981).

exist for other geometric shapes. The drag coefficient includes both drag caused by an unsymmetrical pressure distribution (***form drag***) and drag caused by shear stresses acting on the sphere's surface (***viscous drag***). The marked reduction in drag on a sphere at a Reynolds number around 200,000 is caused by transition from laminar to turbulent boundary layer flow separation (delayed flow separation) on the downstream side of the sphere; this sudden decrease in drag is sometimes called the ***drag crisis***. It is common practice to divide the flow into five flow regimes, as labeled in Figure 8.11:

- ***Stokes flow regime***: $Re < 10^{-1}$ $c_D \approx 24/ Re$
- ***Transitional flow regime***: $10^{-1} < Re < 10^3$ c_D = variable
- ***Newtonian flow regime***: $10^3 < Re < 10^5$ $c_D \approx 0.4$
- ***Transitionally turbulent flow regime***: $10^5 < Re < 10^6$ c_D = variable
- ***Fully turbulent flow regime***: $10^6 < Re$ $c_D \approx 0.2$

Reynolds number is defined in terms of the relative velocity and the particle diameter,

$$\boxed{Re = \frac{\rho D_p \left|\vec{v} - \vec{U}\right|}{\mu} = \frac{\rho D_p \left|\vec{v}_r\right|}{\mu} = \frac{D_p \left|\vec{v}_r\right|}{\nu} = \frac{D_p v_r}{\nu}} \qquad (8\text{-}58)$$

where μ is the ***dynamic viscosity*** and $\nu = \mu/\rho$ is the ***kinematic viscosity***. The relationship between sphere drag coefficient and Reynolds number for $Re < 10^5$ can be expressed by the following empirical equation with an accuracy of around 10%:

$$\boxed{c_D = 0.4 + \frac{24}{Re} + \frac{6}{\left(1 + \sqrt{Re}\right)}} \qquad (8\text{-}59)$$

If the Reynolds number is very small, the Stokes flow equation is adequate, and much simpler to employ:

- $Re < 0.1$: $\boxed{c_D = \frac{24}{Re}}$ (8-60)

If Re is larger than 0.1, but the range of Reynolds numbers in an application is narrow, the following empirical expressions are suggested by Willeke and Baron (1993):

- $0.1 < Re < 5$: $\boxed{c_D = \frac{24}{Re}\left(1 + 0.0916\,Re\right)}$ (8-61)
- $5 < Re < 1000$: $\boxed{c_D = \frac{24}{Re}\left(1 + 0.158\,Re^{2/3}\right)}$ (8-62)

It must be emphasized that the speed used in the Reynolds number is based on the *relative* speed (v_r) between the particle and the fluid, as defined by Eq. (8-56). For particles moving in motionless air, the relative velocity *is* the particle velocity. For particles traveling through a moving fluid, great care must be taken to evaluate the relative velocity.

Either the dynamic viscosity (μ) or the kinematic viscosity (ν) of the carrier gas must be known in order to calculate Re in Eq. (8-58). For most gases, μ is a strong function of temperature, but a very weak function of pressure. For air, the dynamic viscosity can be expressed empirically as a function of temperature (T), in units of kg/(m s). A well-known, highly accurate equation for μ as a function of T is ***Sutherland's law***,

$$\boxed{\mu = \mu_0 \left(\frac{T}{T_0}\right)^{1.5} \left(\frac{T_0 + S}{T + S}\right)} \qquad (8\text{-}63)$$

where $\mu_0 = 1.71 \times 10^{-5}$ kg/(m s), $T_0 = 273.15$ K, S = 110.4 K, and T must be in units of K. Other (less accurate) equations for μ can be obtained by performing a least-squares polynomial fit of experimental data; e.g. the following third-order polynomial fit (from Appendix A.11):

$$\boxed{\mu = \left(1.3554\times10^{-6} + 0.6738\times10^{-7}\,T - 3.808\times10^{-11}T^2 + 1.183\times10^{-14}T^3\right)\ \frac{kg}{m\ s}} \qquad (8\text{-}64)$$

where T must again be in units of K. The kinematic viscosity (ν) can be calculated from either of these by definition, $\nu = \mu/\rho$. Shown in Figure 8.12 are μ and ν for air as functions of temperature at standard pressure. The values calculated by Eq. (8-64) overlap those calculated by Eq. (8-63) except at large values of T, where the polynomial curve fit deviates from Sutherland's law.

Air consists of molecules that travel at very high speed. The average distance traveled by air molecules between collisions with each other is called the ***mean free path*** (λ). Mean free path can be expressed in terms of viscosity by the following equation (Jenning, 1988; Flagan and Seinfeld, 1988):

$$\boxed{\lambda = \frac{\mu}{0.499\sqrt{\frac{\pi}{8}}\sqrt{\rho P}}} \qquad (8\text{-}65)$$

For air at STP, $\mu_{STP} = 1.830 \times 10^{-5}$ kg/(m s), $\rho_{STP} = 1.184$ kg/m^3, $P_{STP} = 101{,}325$ Pa, and $\lambda_{STP} = 0.06635$ μm. Assuming air to be a ideal gas (often called a perfect gas),

$$\boxed{P = \rho\frac{R_u}{M}T = \rho RT} \qquad (8\text{-}66)$$

where R_u is the universal gas constant, and R is the specific gas constant, as defined in Chapter 1. The mean free path at temperatures and pressures other than STP can be expressed as

$$\boxed{\lambda(T,P) = \lambda_{STP}\left(\frac{\mu}{\mu_{STP}}\right)\left(\frac{P_{STP}}{P}\right)\sqrt{\frac{T}{T_{STP}}}} \qquad (8\text{-}67)$$

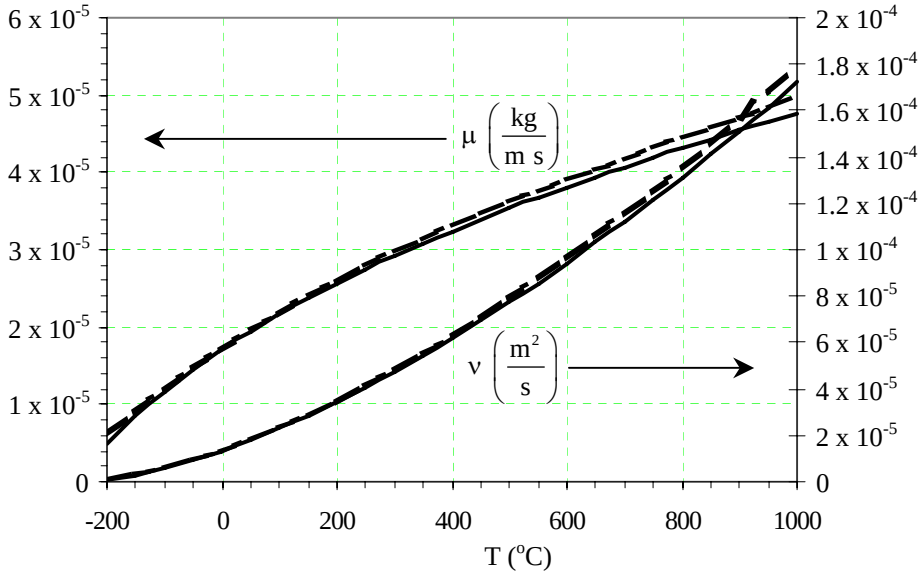

Figure 8.12 Dynamic viscosity (μ) and kinematic viscosity (ν) of air as functions of temperature at standard atmospheric pressure; solid line from Eq. (8-63), dashed line from Eq. (8-64).

A fluid is considered a continuum fluid if the moving particle is considerably larger than the mean free path of the fluid; the particle moves through the fluid as if the fluid were a continuous medium. On the other hand, if the particle is comparable in size (or smaller) than the mean free path, the particle is affected by collisions with individual molecules, and at times slips between molecules. Such motion is called ***free molecular flow*** or more generally, ***slip flow***.

The parameter used to distinguish the continuum regime from the free molecular regime is the Knudsen number (Kn), defined as the ratio of the mean free path to a characteristic length of the particle. For spherical particles,

$$\boxed{\mathrm{Kn} = \frac{\lambda}{D_p}} \tag{8-68}$$

Three regimes can be classified according to the value of the Knudsen number as follows:

- Kn < 0.1 ***continuum regime***
- 0.1 < Kn < 10 ***transitional flow regime***
- Kn > 10 ***free molecular flow regime***

Note that since particle diameter is in the denominator of Eq. (8-68), smaller particles have larger Knudsen numbers. Note also that the "transitional flow regime" defined here is not the same as the transitional flow regime defined previously for drag on a sphere.

Engineers are familiar with the equations of continuum fluid mechanics, but many contaminant particles, e.g. smoke, fume, or fine dust, are in the transitional or free molecular flow regimes. When dealing with these particles, one must modify Eq. (8-55). It is expedient and accurate to insert a parameter called the ***Cunningham slip factor*** (C), also called the ***Cunningham correction factor*** or simply the ***slip factor***, into the denominator of the equation for aerodynamic drag. The slip factor can be expressed by the following (Jenning, 1988):

$$\boxed{\mathrm{C} = 1 + \mathrm{Kn}\left[2.514 + 0.80\exp\left(-\frac{0.55}{\mathrm{Kn}}\right)\right]} \tag{8-69}$$

For spherical particles, Eq. (8-55) thus becomes

$$\boxed{\vec{F}_{drag} = -c_D \frac{\rho}{2C}\frac{\pi D_p^{\,2}}{4}\left(\vec{v}-\vec{U}\right)\left|\vec{v}-\vec{U}\right| = -c_D \frac{\rho}{2C}\frac{\pi D_p^{\,2}}{4}\vec{v}_r\left|\vec{v}_r\right|} \tag{8-70}$$

The relationship between the slip factor and the diameter of spherical particles in air at STP is shown in Table 8.4.

Table 8.4 Knudsen number and Cunningham correction factor for spherical particles in air at STP.

D_p (μm)	Kn	C
0.001	66.37	220.5
0.002	33.19	110.5
0.005	13.27	44.56
0.01	6.637	22.57
0.02	3.319	11.59
0.05	1.327	5.039
0.1	0.6637	2.900
0.2	0.3319	1.885

D_p (μm)	Kn	C
0.5	0.1327	1.335
1	0.0664	1.167
2	0.0332	1.083
5	0.0133	1.033
10	0.0066	1.017
20	0.0033	1.008
50	0.0013	1.003
100	0.0007	1.002

It is clear that for large particles, $D_p >> \lambda$, the slip factor (C) is essentially unity and can be omitted from Eq. (8-70). The slip factor is particularly significant for submicron particles. It should be noted that the slip factor is independent of particle velocity, but depends only on particle size and the physical properties of the fluid.

8.4.3 Effect of Particle Shape on Aerodynamic Drag

Particles vary in geometry, e.g. perfect spheres such as condensed vapors, cylindrical or flat filaments such as cotton fibers or asbestos in which the ratio of length to width is large, platelets such as silica or mica, feathery agglomerates such as soot, and irregularly shaped fragments such as coal dust, foundry sand, or metal grinding particles. If particles are not spheres the drag may be quite different than for spheres of the same mass. To accommodate nonspherical particles, Fuchs (1964) suggested introducing a unitless ***dynamic shape factor*** (X, Greek letter chi), defined as the ratio of the drag force of the nonspherical particle and the drag force of a sphere having the same volume and velocity. Thus the drag force of Eq. **Error! Reference source not found.** is further modified for nonspherical particles as

$$\boxed{\vec{F}_{drag} = -Xc_D \frac{\rho}{2C} \frac{\pi D_{e,p}^{\ 2}}{4} \left(\vec{v} - \vec{U}\right) \left|\vec{v} - \vec{U}\right| = -Xc_D \frac{\rho}{2C} \frac{\pi D_{e,p}^{\ 2}}{4} \vec{v}_r \left|\vec{v}_r\right|} \qquad (8\text{-}71)$$

where $D_{e,p}$ is the ***equivalent volume diameter*** defined in terms of the actual particle volume (V_p) as

$$\boxed{D_{e,p} = \left(\frac{6V_p}{\pi}\right)^{\frac{1}{3}}} \qquad (8\text{-}72)$$

and the drag coefficient is expressed in terms of the Reynolds number based on this equivalent volume diameter. The Cunningham correction factor should also be computed on the basis of the equivalent volume diameter. The equivalent volume diameter is the diameter an actual particle would have if it were a sphere. For flow beyond the Stokes flow regime, one may use Eq. (8-71) to describe the drag in lieu of a better expression, but readers are urged to consult other sources (Fuchs, 1964; Davies, 1966; Strauss, 1966; Hidy and Brock, 1970; Hinds, 1982; Cheng et al., 1988; Lee and Leith, 1989) for more details. Table 8.5 shows values of the dynamic shape factor (X) for a variety of common shapes. Dynamic shape factors for particles that have a length, width, and height of comparable value are close to unity, and may be omitted for purposes of indoor air pollution analysis. For these cases, $D_{e,p}$ may be replaced by either the length, width, or height. Leith (1987) suggests that the dynamic shape factor (X) can be estimated as follows:

$$\boxed{X = \left(0.33 + 0.67 \frac{D_{s,p}}{D_{p,p}}\right) \frac{D_{e,p}}{D_{p,p}}} \qquad (8\text{-}73)$$

where $D_{p,p}$ and $D_{s,p}$ are called the ***equivalent projected area diameter*** and ***equivalent surface area diameter*** respectively,

- $D_{p,p}$ = diameter of a sphere with the same projected area as the actual particle, where projected area is the cross-sectional area of the particle normal to the direction of flow
- $D_{s,p}$ = diameter of a sphere with the same surface area as the actual particle

Sauter mean diameter is defined as the total volume of all particles in an aerosol divided by the total surface area of all the particles. From this definition, Sauter diameter can be thought of as a mean volume-to-surface diameter.

Spherical particles whose density is equal to 1000 kg/m^3, the density of water, are called ***unit density spheres***. Such particles have a ***specific gravity*** (SG) equal to 1.0, where SG is defined as the ratio of particle density (ρ_p) to water density (ρ_{water}),

Table 8.5 Dynamic shape factors, averaged over all orientations unless otherwise noted (abstracted from Fuchs, 1964 and Strauss, 1966).

shape		X
sphere		1.00
cube		1.08
cylinder (L/D = 4):		
	axis horizontal	1.32
	axis vertical	1.07
ellipsoid, across polar axis, with ratio of major to minor diameters = 4		1.20
parallelepiped with square base, with various values of height to base:		
	0.25	1.15
	0.50	1.07
	2.00	1.16
	3.00	1.22
	4.00	1.31
clusters of spheres		
	chain of 2	1.12
	chain of 3	1.27
	3 compact	1.15
	chain of 4	1.32
	4 compact	1.17

$$SG = \frac{\rho_p}{\rho_{water}} \tag{8-74}$$

For the most part, the density of a particle is the density of the compound of which it is composed. In the event the particle contains voids, is a loose feathery agglomerate, or is a composite material, the density is more difficult to define. Details of how to cope with these circumstances can be found in Hinds (1982).

8.4.4 Predicting the Trajectory of a Spherical Particle

For a spherical particle of diameter D_p, the net gravitational force is given by Eq. (8-54), and the drag force is given by Eq. (8-70). Substitution of these expressions into Eq. (8-52) yields the equation of motion of a single spherical particle in air,

$$\pi\frac{D_p^{\,3}}{6}\rho_p\frac{d\vec{v}}{dt} = \pi\frac{D_p^{\,3}}{6}\vec{g}\left(\rho_p-\rho\right) - c_D\frac{\rho}{2C}\pi\frac{D_p^{\,2}}{4}\left(\vec{v}-\vec{U}\right)\left|\vec{v}-\vec{U}\right| \tag{8-75}$$

Consider the general motion of a spherical particle traveling in the x-y plane through a moving two- dimensional gas stream in which air velocity $\vec{U}$ varies, and in which the gravity vector is in the negative y direction. Let the particle have initial velocity $\vec{v}(0)$. Figure 8.10 depicts such motion. Equation (8-75) reduces to

$$\frac{d\vec{v}}{dt} = -\hat{j}g\frac{\rho_p-\rho}{\rho_p} - \frac{3\rho c_D}{4C\rho_p D_p}\left(\vec{v}-\vec{U}\right)\left|\vec{v}-\vec{U}\right| \tag{8-76}$$

where

$$\boxed{\left(\vec{v}-\vec{U}\right)=\hat{i}\left(v_x-U_x\right)+\hat{j}\left(v_y-U_y\right)=\hat{i}v_{rx}+\hat{j}v_{ry}} \tag{8-77}$$

and

$$\boxed{v_r=\left|\vec{v}-\vec{U}\right|=\sqrt{v_{rx}{}^2+v_{ry}{}^2}} \tag{8-78}$$

The above reduces to a pair of coupled differential equations,

$$\boxed{\frac{dv_x}{dt}=-\frac{3c_D\rho}{4C\rho_p D_p}v_{rx}\sqrt{v_{rx}{}^2+v_{ry}{}^2}} \tag{8-79}$$

and

$$\boxed{\frac{dv_y}{dt}=-g\frac{\rho_p-\rho}{\rho_p}-\frac{3c_D\rho}{4C\rho_p D_p}v_{ry}\sqrt{v_{rx}{}^2+v_{ry}{}^2}} \tag{8-80}$$

where drag coefficient (c_D) is a function of Reynolds number, as in Eqs. (8-59) through (8-62). The Reynolds number of Eq. (8-58) reduces to

$$\boxed{\mathrm{Re}=\frac{\rho D_p\sqrt{v_{rx}{}^2+v_{ry}{}^2}}{\mu}=\frac{\rho D_p v_r}{\mu}=\frac{D_p v_r}{\nu}} \tag{8-81}$$

8.4.5 Particle Trajectory in the Stokes Flow Regime

If the particle's motion is entirely within the Stokes flow regime, Eq. (8-60) applies; replacing c_D by 24/Re *decouples* Eqs. (8-79) and (8-80), resulting in a simplified set of uncoupled equations,

$$\boxed{\frac{dv_x}{dt}=-\frac{\left(v_x-U_x\right)}{\tau_p C}} \tag{8-82}$$

and

$$\boxed{\frac{dv_y}{dt}=-g\frac{\rho_p-\rho}{\rho_p}-\frac{\left(v_y-U_y\right)}{\tau_p C}} \tag{8-83}$$

where τ_p is called the ***particle relaxation time*** since it possesses the units of time, and because it is customary to use this name when it appears in first-order differential equations like Eq. (8-82) or (8-83). τ_p is defined as

$$\boxed{\tau_p=\frac{\rho_p D_p{}^2}{18\mu}} \tag{8-84}$$

Thus if U_x and U_y are constant or known functions of x and y, Eqs. (8-82) and (8-83) can be solved to predict v_x and v_y as functions of time and known initial conditions, $v_x(0)$ and $v_y(0)$.

To illustrate this kind of Stokes flow, consider the case in which a particle enters an air stream that is moving to the right at constant speed U. (The components of the air velocity are U_x = U and U_y = 0.) The particle's initial velocity components are $v_x(0)$ and $v_y(0)$, which are arbitrary. Shown in Figure 8.13 is the particle at some arbitrary time, along with the forces acting on it. Equations (8-82) and (8-83) become simple first-order ordinary differential equations with constant coefficients. It is left as an exercise for the reader to rewrite these equations in standard form, i.e. in the form of Eq. (1-59), for which analytical solutions are possible. The solutions are

$$\boxed{v_x(t)=v_x(0)\exp\left(-\frac{t}{\tau_p C}\right)+U\left[1-\exp\left(-\frac{t}{\tau_p C}\right)\right]} \tag{8-85}$$

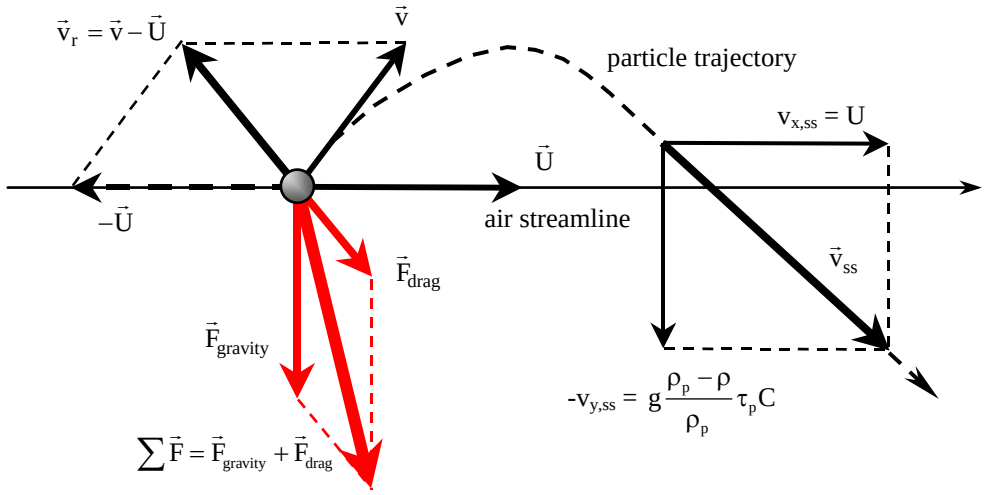

Figure 8.13 Particle moving through air, which is moving horizontally; forces on the particle and the particle trajectory are shown.

and

$$v_y(t) = v_y(0)\exp\left(-\frac{t}{\tau_p C}\right) - Cg\frac{\rho_p - \rho}{\rho_p}\tau_p\left[1 - \exp\left(-\frac{t}{\tau_p C}\right)\right] \tag{8-86}$$

After some time, $t >> \tau_p$, the transients can be neglected, and the particle maintains a steady-state velocity, $\vec{v}_{ss}$, as also shown in Figure 8.13. Equations (8-85) and (8-86) reduce to

$$\vec{v}_{ss} = \vec{v}_{steady\ state} = U\cdot\hat{i} + \left(-g\frac{\rho_p - \rho}{\rho_p}\tau_p C\right)\cdot\hat{j} \tag{8-87}$$

The net force on the particle in steady-state conditions is zero as shown in Figure 8.14.

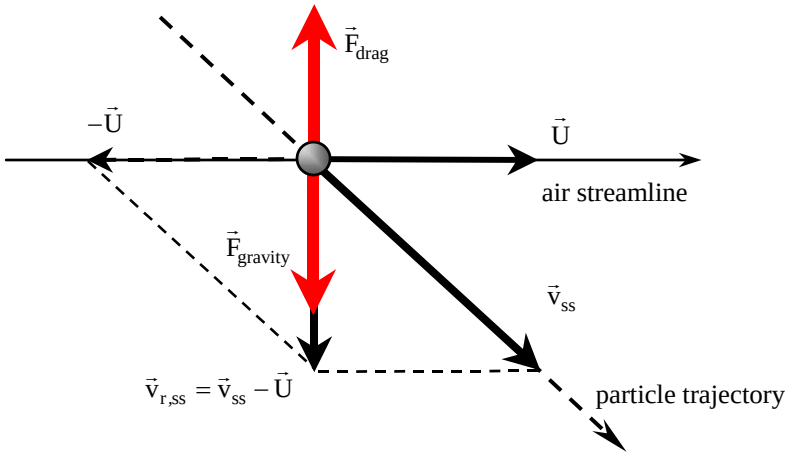

Figure 8.14 Particle moving through air, which is moving horizontally; the forces acting on the particle and the particle trajectory are shown for steady-state conditions.

As shown, the aerodynamic drag force is vertical, exactly balancing the gravitational force. By Newton's law, the particle experiences no further acceleration – it moves in a straight diagonal line at constant speed as sketched. This analysis justifies the commonplace assumption that small particles move horizontally at a speed equal to the carrier gas, and simultaneously drift downward relative to the gas at a speed equal to the ***terminal settling velocity*** (v_t), sometimes simply called the ***terminal velocity*** or the ***fall velocity***. In the case being examined here,

$$\boxed{v_t = -v_{y,ss} = Cg\frac{\rho_p - \rho}{\rho_p}\tau_p} \tag{8-88}$$

One must keep in mind that this is true only for spherical particles in Stokes flow, and is only an approximation for other flow regimes. This behavior is often assumed as a general proposition, which may be adequate providing the accuracy requirements (or lack thereof) of the analysis allow it.

If the Reynolds numbers are unknown and one suspects that the flow is apt to be beyond the Stokes flow regime, differential equations (8-79) and (8-80) remain coupled and numerical methods are required to compute the particle velocity and trajectory. For brevity, only two-dimensional motion is described. To solve these equations numerically, they are first rewritten in standard form for first-order ordinary differential equations,

$$\boxed{\frac{dv_x}{dt} = B_x - A_x v_x \qquad \text{and} \qquad \frac{dv_y}{dt} = B_y - A_y v_y} \tag{8-89}$$

where, since $v_{rx} = v_x - U_x$ and $v_{ry} = v_y - U_y$,

$$\boxed{A_x = A_y = \left(\frac{3c_D\rho}{4C\rho_p D_p}\right)\sqrt{\left(v_x - U_x\right)^2 + \left(v_y - U_y\right)^2}} \tag{8-90}$$

$$\boxed{B_x = A_x U_x} \tag{8-91}$$

and

$$\boxed{B_y = A_y U_y - g\frac{\rho_p - \rho}{\rho_p}} \tag{8-92}$$

In the general case, air velocity components (U_x and U_y) change with location (x and y) as the particle moves. Thus, two additional equations need to be solved to predict the trajectory, namely

$$\boxed{v_x = \frac{dx}{dt} \quad \text{and} \quad v_y = \frac{dy}{dt}} \tag{8-93}$$

Four coupled ordinary differential equations, Eqs. (8-89) and Eqs. (8-93), must be solved simultaneously. This is accomplished by numerical means; the ***Runge-Kutta method*** (Appendix A.12) is recommended.

Example 8.5 - Trajectory of Particles in a Boundary Layer

Given: In a production line, a high-speed press punches holes in a strip of metal ribbon that is formed into electrical connectors for the automotive industry. The speed of the operation requires the metal to be bathed in cutting oil (ρ = 891. kg/m^3) to cool and lubricate the punch. Insufficient local ventilation is provided and drops of cutting oil are ejected upward into the air with an initial velocity of around 30. m/s at an angle approximately 150^o from the positive x-axis. The injection point is x = 0.0, y = 1.0 cm. The range of particle diameters is estimated to be 50 μm < D_p < 200 μm. Room air passes over the horizontal surface as a boundary layer in the positive x-direction with horizontal velocity component approximated by

$$U_x = U_\infty \sin\left(\frac{y}{\delta}\right)$$

where U_∞ = 5.0 m/s and δ is the boundary layer thickness, which is equal to 10. cm. Above the boundary layer thickness ($y > \delta$), $U_x = U_\infty$ = constant. The air has negligible vertical velocity component. The workers claim that the large drops are carried far downwind while small particles are not. The plant engineer claims that that they are wrong – the large particles should settle close to where they are injected because of their weight, and no particles will be transported beyond about one meter from the point of injection.

To do: Use a numerical technique to predict the velocity and trajectory of these oil particles traveling in the given air stream.

Solution: The authors used Mathcad to perform Runge-Kutta marching. Trajectories for the two extreme particle diameters (D_p = 50 and 200 μm) are shown in Figure E8.5. The 50 μm particles settle at around 0.74 m downstream of the injection site, while the 200 μm particles settle much further downstream, at about 1.8 m.

Discussion: The results show that the workers are right and the plant engineer is wrong. Unlike trajectories in air moving uniformly in the x-direction, the calculations show that large particles travel the farthest. The reason for this behavior is that large particles possess more inertia, and rise to greater values of y before their upward motion is damped by aerodynamic drag and gravity. At these large values of y, the larger particles encounter higher air velocities that sweep them farther downwind than the smaller particles. As seen in Figure E8.5, the 50 μm particles never rise above the boundary layer, which is 0.10 m high.